Proceedings of the Fourth International Conference

Path Integrals from meV to MeV: Tutzing '92

Tutzing, Bavaria May 18–21, 1992

Editors

Hermann Grabert
Akira Inomata
Lawrence S. Schulman
Ulrich Weiss

World Scientific
Singapore • New Jersey • London • Hong Kong

SEMICLASSICAL QUANTIZATION OF THE HELIUM ATOM

K. RICHTER, G. TANNER, AND D. WINTGEN

Fakultät für Physik, Hermann-Herder-Str. 3, 7800 Freiburg, FRG

ABSTRACT

We report on recent investigations of the classical and semiclassical properties of the helium atom. We show that regular as well as chaotic classical motion of the electrons exists. Semiclassically, both types of motion require a separate treatment. Stability islands in phase space are quantized via a torus-quantization-type procedure, whereas a periodic-orbit cycle expansion approach accounts for the states associated with chaotic electron pair motion. The results are compared with accurate *ab initio* quantum calculations.

1. Introduction

Nowadays, a proper semiclassical treatment of the helium atom is still an outstanding problem of semiclassical theory. This is due to the fact that the Hamiltonian contains at least three non-separable degrees of freedom. As we will show, the classical phase space of the two-electron system is of mixed structure, i.e. regular and irregular motion of the electron pair co-exists. Due to the high dimensionality of the problem and the complex phase space structure no semiclassical methods exist at the present which would allow for a uniform quantization of the classical (periodic) motion. The helium atom therefore remains one essential touchstone of semiclassical mechanics, even though considerable progress in the development of the formal theory has been achieved within the last years [1].

A semiclassical description of two-electron atoms is also highly desirable, because most parts of the spectral regions are still unexplored, both experimentally and quantum theoretically.

2. Methods

2.1 *Classical mechanics*

For the three body Coulomb problem there exist only the total angular momentum $\mathbf{L}$ and the total energy E as constants of motion. Here we will focus on states with total angular momentum $\mathbf{L} = 0$, for which the motion of the electrons is confined to a fixed plane in configuration space. This removes three of the total of six degrees of freedom, and we take the three inter-particle distances r_i as dynamical variables.

For a nucleus with charge Z and infinite mass the Hamiltonian reads (atomic units used, $e = m_e = 1$):

$$H = \frac{\mathbf{p}_1^2 + \mathbf{p}_2^2}{2} - \frac{Z}{r_1} - \frac{Z}{r_2} + \frac{1}{r_{12}} . \tag{1}$$

The electron-nucleus distances are given by r_i, $i = 1, 2$, and the distance between the electrons is r_{12}. Whenever an inter-particle distance vanishes (particle collision) the potential energy diverges. Therefore an essential ingredient for the classical analysis of the three-body Coulomb problem is the regularization of the equations of motion. A numerically convenient

method to regularize the binary collisions can be found in Ref. [2].

The Hamiltonian is homogeneous in coordinates and momenta and the equations of motion can be scaled to energy independent form. The accumulated action along a classical path is then $\tilde{S}(E) = 2\pi z S$ with $z = (-E)^{-1/2}$ and $2\pi S$ the action at energy $E = -1$.

2.2. *Semiclassical Quantization*

The connection between the quantum eigenvalues and periodic orbits was obtained by Gutzwiller [1] starting from the relation between the density of states ρ and the trace of the Green function G, $\rho(E) = -\frac{1}{\pi}\mathrm{Im\ tr}\, G$. By using a semiclassical approximation of Feynman's path-integral formalism Gutzwiller obtained a representation of the Green function, i.e. the density of states in terms of classical periodic orbits. The level density $\rho = \rho_0 + \rho_{osc}$ is composed of a smooth part ρ_0 and oscillatory contributions ρ_{osc} due to periodic orbits. The leading contribution (in $\hbar$) to ρ_0 is given by the size of the energy shell. We focus on the oscillatory part ρ_{osc}, which turns out to be a sum over all contributions of different *primitive* (i.e. non-repeated) periodic orbits (PPO) and multiple transversals (given by the index r) [1]

$$\frac{-i}{\hbar} T_p \sum_{r=1}^{\infty} \frac{e^{(iS_p/\hbar - i\mu_p\pi/2)r}}{|\det(M^r - 1)|^{1/2}}. \tag{2}$$

In Equation (2) $S_p = \int_{ppo} \mathbf{p}\, d\mathbf{q}$ is the accumulated action along a PPO, T_p the time for one transversal and $\mathbf{M}$ the stability matrix associated with the PPO. The phase shift μ_p is the Morse index of the PPO. The stability character of each periodic orbit determines its weight and therefore its spectral significance. The trace formula opens the principal possibility for the calculation of semiclassical energies, although the evaluation of the sum over the contributions (2) depends on the specific structure of classical phase space.

2.3. *Quantum mechanical ab-initio calculations*

Our numerical method to solve the Schrödinger equation for highly doubly-excited electron states can be found, e.g., in Ref. [3]. We obtain resonance positions and resonance widths within near-machine precision even for highly doubly excited states [3]. This allows us to check very accurately the predictions of the classical, semiclassical methods described in the previous sections.

3. Results

For total angular momentum $\mathbf{L} = \mathbf{0}$ the (three dimensional) electronic motion in the helium atom is confined to a plane fixed in configuration space. However, there exist special symmetry planes where the electronic motion becomes essentially two-dimensional: Motion on the so-called Wannier ridge takes place in the $r_1 = r_2$ plane but turns out to be (except for the so-called Langmuir orbit) extremely unstable and of minor importance for the corresponding quantum system. The other two symmetry planes $\Theta = \pi, 0$ (where Θ is the angle between the electron radius vectors) characterize collinear motion with both electrons localized on different sides or on the same side of the nucleus, respectively.

In the following we apply semiclassical quantization to the motion in the two-dimensional symmetry planes. The third degree of freedom is taken into account by linearizing the equations of motion perpendicular to the symmetry planes.

3.1. *The $Z^{2+}e^-e^-$ configuration*

Consider a collinear arrangement of a nucleus of charge Z and of two electrons, both being on the same side of the nucleus. The fundamental periodic motion of such a configuration is a coherent oscillation of both electrons with the same frequency but, as it turns out, with large differences in their individual radial amplitudes and velocities as shown in figure 1(a) for helium ($Z = 2$). The outer electron appears to stay nearly frozen at some fixed radial distance. For this reason we label the orbits as *frozen planet configurations*. The minimal nuclear charge to bind an electron in this type of collinear configuration is $Z > 1$; otherwise the outer electron potential is purely repulsive. The configurations considered here cannot be described within an independent particle model and are of highly non-perturbative nature.

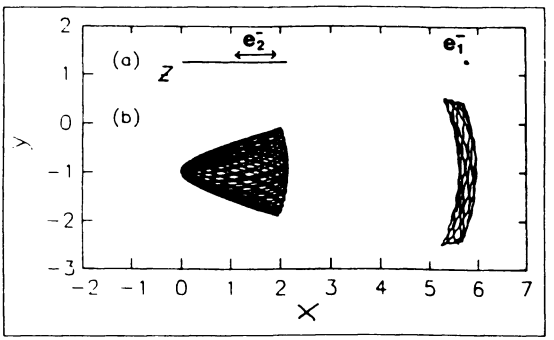

Figure 1:
(a) The straight line motion of the electron pair for the frozen planet PO, while a non-periodic but regular trajectory in its neigborhood is shown in (b). Energy scaled units $(-E)r$ are used.

Most remarkably, the periodic orbit (PO) of Figure 1(a) is linearly stable with respect to variations in the initial conditions. This is demonstrated in figure 1(b) which shows the resulting (regular) motion of the electrons when they are initially in a slightly off-collinear arrangement. The inner electron moves on perturbed Kepler ellipses around the nucleus, while the outer electron remains trapped at large radial distances following the slow angular oscillations of the inner electron. As is shown in Ref. [3] the PO of Figure 1(a) is also stable with respect to variations in the initial conditions within the subspace of collinear motion.

The two corresponding pairs of eigenvalues of the stability matrix M are then complex numbers on the unit circle, i.e. $\lambda_R = \exp(\pm 2\pi i \gamma_R)$ and $\lambda_\Theta = \exp(\pm 2\pi i \gamma_\Theta)$. For trajectories close to the periodic orbit the frequency ratios of the radial and angular motion transverse to the periodic orbit are given by the winding numbers $\gamma_R = 0.0677$ and $\gamma_\Theta = 0.4616$, respectively. Expanding the determinant in Eq. (2) into geometric series, the contribution (2) of the frozen planet periodic orbit to the density of states is

$$\rho_{fpo} \sim \sum_{r=1}^{\infty} \sum_{k,l=0}^{\infty} \exp 2\pi i r \left(\frac{S}{\hbar} - \frac{\mu'}{4} - (l + \frac{1}{2})\gamma_R - 2(k + \frac{1}{2})\gamma_\Theta\right), \qquad (3)$$

where the number of conjugate points along the trajectory are already contained in the winding number.

The sum over the repetitions r in (3) is a geometric series which can be summed analytically. Using the classical scaling property for the action Eq. 3 results in a triple-Rydberg

formula for the energies converging to the three-body breakup threshold [3],

$$E_{nkl} = -\frac{S^2}{(n+\frac{1}{2}+(l+\frac{1}{2})\gamma_R+(2k+1)\gamma_\Theta)^2}, \tag{4}$$

with $S = 1.4915$ the scaled action of the periodic orbit. The semiclassical quantum numbers n, k and l reflect the approximate separability of the associated semiclassical wave functions in the local coordinates $\{q_i\}$ of the periodic orbit. Nodal excitations along the orbit are described by n, whereas k and l count the excitations perpendicular to the orbit.

Table 1: Energies of the $(n,0,0)$ configurations obtained by full quantum solutions (singlet ($^1S^e$) and triplet ($^3S^e$) states respectively) and the semiclassical triple Rydberg formula (2) (E_{scl}). In addition the total decay widths obtained from complex rotation are given.

n	$-E\,(^1S^e)$	$\Gamma/2\,(^1S^e)$	$-E\,(^3S^e)$	$\Gamma/2\,(^3S^e)$	E_{scl}
2	0.257 371 609	0.000 010 564	0.249 964 615	0.000 006 789	0.247 923
3	0.141 064 156	0.000 011 739	0.140 088 483	0.000 004 409	0.139 351
4	0.089 570 804	0.000 002 024	0.089 467 826	0.000 000 179	0.089 144
5	0.062 053 558	0.000 000 560	0.062 041 278	0.000 000 033	0.061 887
6	0.045 538 667	0.000 000 202	0.045 539 242	0.000 000 376	0.045 458
7	0.034 842 642	0.000 000 368	0.034 843 857	0.000 000 143	0.034 798
8	0.027 517 599	0.000 001 184	0.027 519 289	0.000 000 022	0.027 491
9	0.022 284 587	0.000 000 525	0.022 283 665	0.000 000 035	0.022 265
10	0.018 411 985	0.000 000 058	0.018 411 896	0.000 000 030	0.018 400
11	0.015 468 259	0.000 000 023	0.015 468 265	0.000 000 019	0.015 460
12	0.013 178 121	0.000 000 022	0.013 178 140	0.000 000 010	0.013 172
13	0.011 361 442	0.000 000 014	0.011 361 444	0.000 000 005	0.011 357
14	0.009 896 121	0.000 000 004	0.009 896 120	0.000 000 002	0.009 893

Table 1 summarizes the positions and widths of frozen planet resonances $(n, k{=}0, l{=}0)$ with n ranging from 2 to 14 together with the predictions of the simple semiclassical formula (4). Considering the rather large basis sets necessary to obtain the accurate quantum results (up to $\sim$ 7000 basis states used) the accuracy of the semiclassical results, which are obtained on a pocket calculator, are rather impressive.

A direct examination of the nodal structure of the associated wave functions is a more stringent test than comparing energy eigenvalues. Figure 2(a) depicts the conditional probability distribution of the wave function for the $(6,0,0)$-state for the collinear arrangement $r_{12} = r_1 - r_2$. The off-collinear part of the probability density, not shown here, decreases exponentially indicating a zero-point motion in the bending degree of freedom. This zero-point motion is expressed by the assignment $k = 0$. The coordinate r_1 (r_2) denotes the radial distance of the outer (inner) electron. The outer electron probability is strongly localized in the region $r_1 \approx 125$, reflecting the classical localization of the 'frozen' electron. Note also the large differences in the radial extents r_i. The nodal excitations are all directed along the frozen planet PO, which is a nearly straight line along the frozen-planet radius indicated by an arrow in the figure. Recalling the typical quadratic spacing of nodal lines in Coulombic systems, we achieve nearly constant nodal distances by using quadratically scaled axes as

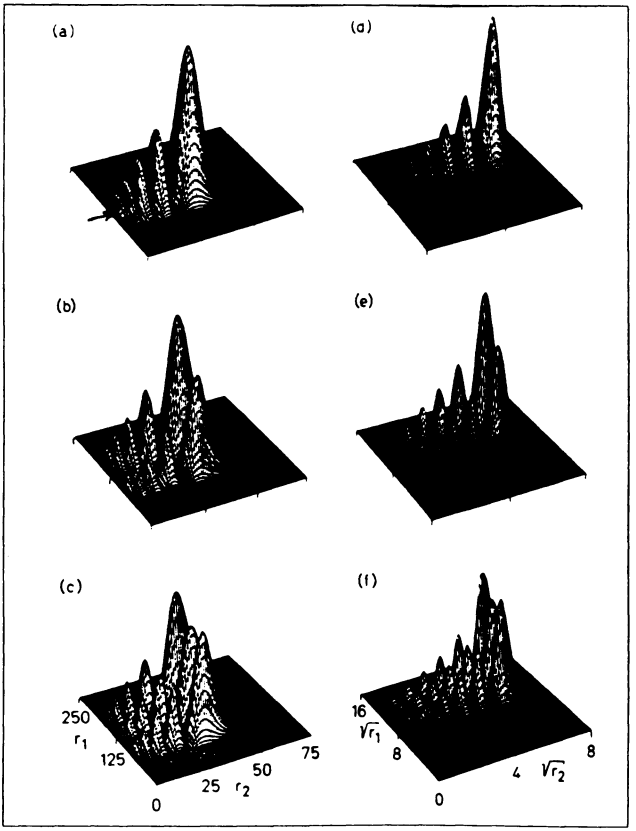

Figure 2:
Conditional probability densities of $(n,0,l)$ states in helium for n=6. The angle Θ between $\mathbf{r}_1$ and $\mathbf{r}_2$ is fixed to Θ=0. The axes have a linear (left part) and a quadratic scale (right part), respectively. Shown are l=0 (a,d), l=1 (b,e), and l=2 (c,f). Note the asymmetry in the scales of the axes. Only the parts $r_1 > r_2$ are shown. The full wavefunction is symmetric in r_1 and r_2.

done in part (d). The number of nodes along the orbit is 6 in agreement with the semiclassical predictions. The wave function only has a zero-point distribution perpendicular to the orbit (in the symmetry plane of collinear motion), which agrees with the semiclassical local coordinate classification $(n,k,l) = (6,0,0)$.

Wavefunctions with nodal excitations transverse to the orbit preserving the collinear character of the (quantum) motion are shown in parts (b), (e) and (c), (f) of Figure 2. They correspond to the $l = 1$ and $l = 2$ nodal excitations of the $n = 6$ manifold of states. Their energies differ only slightly due to the small winding number γ_R.

3.2 *The $e^-Z^{2+}e^-$ configuration*

Configurations where the electrons move on opposite sides of the nucleus are energetically favored because the electron–electron interaction is minimized. Quantum mechanically, these are the (resonant) states in which $-\langle\cos\Theta\rangle$ is close to unity. These states are dominantly excited in single-photon transitions from the ground state [6].

The classical motion of the collinear helium atom with the electrons on different sides of the nucleus turns out to be fully chaotic, even though we cannot rigorously prove this. A system is called "chaotic" if all PO are linearly unstable and their number proliferates exponentially with the action (or some other length characteristic). The exponential proliferation becomes obvious if the PO can be mapped onto a tree of symbols [1, 8]. Our numerical findings on the collinear motion of the helium atom suggest that the PO obey a binary coding. As discussed in detail in Ref. [5] all PO of the collinear system can be mapped one–to–one onto strings of the binary symbols $\{+,-\}$ according to successive electron collisions with the nucleus.

All the orbits are unstable with respect to the motion *within* the collinear arrangement (radial correlation). The linearised motion *off* the symmetry plane (angular correlation) is however stable and characterized by the winding number γ, i.e. the eigenvalues $\exp(\pm 2\pi i\gamma)$ of the stability matrix [9].

Since the classical dynamics for collinear configurations with both electrons on different sides of the atoms turns out to be fully chaotic the (approximate) torus quantization described in the previous section cannot be applied. We now have to sum over the contributions (2) of *all* periodic orbits. Using the product expansion [1, 10] of Gutzwiller's trace formula, we obtain for the present system [5]

$$\prod_n (E - E_n) \sim \prod_{\mathrm{PPO}} \prod_{k=0}^{\infty} \prod_{m=0}^{\infty} (1 - t_{\mathrm{PPO}}^{(k,m)}) . \tag{5}$$

The weight $t_{\mathrm{PPO}}^{(k,m)}$ of each PPO is given by

$$t_{\mathrm{PPO}}^{(k,m)} = (\pm 1)^k a^j \exp[2\pi i z S - i\alpha\pi/2 - (k + \frac{1}{2})u - 4\pi i(m + \frac{1}{2})\gamma] , \tag{6}$$

The plus sign applies to hyperbolic PPO and the minus sign to hyperbolic PPO with reflection.

The formal expression (5) relates the product over quantum eigenvalues with a product over periodic orbits. Unfortunately, the zeros of the right hand side cannot be naively identified with the zeros of the left hand side, because the eigenvalues E_n are located beyond the abscissa of absolute convergence of the rhs.

We use the *cycle expansion* [11] to evaluate the semiclassical expression (5). The idea of the cycle expansion is to expand the infinite product (5) into a power series $\sum_j c_j a^j$ of the bookkeeping index a. For $k = m = 0$ this reads (j equals the symbol length of the PO)

$$\begin{aligned} \prod_{\mathrm{PPO}} (1 - t_{\mathrm{PPO}}) \;&=\; 1 - t_+ - t_- - (t_{+-} - t_+ t_-) \\ &\quad - (t_{++-} - t_+ t_{+-}) - (t_{+--} - t_- t_{+-}) - \ldots \end{aligned} \tag{7}$$

Except for the fundamental orbits '+' and '−' each orbit contribution is accompanied by a compensating term pieced together from shorter orbits. Thus terminating the expansion at a given symbol length effectively means a re–summation of *all* orbits, with the approximation that the longer orbits are shadowed to increasing accuracy by the shorter ones. If each term t_{ab} together with its shadowing term $t_a t_b$ is viewed as a *single* entry d_{ab} then the series (7) converges absolutely.

The products over k and m in (5) originate from the expansion of the Gutzwiller amplitudes (2) into geometric series [10]. They have to be treated differently, because the stability characteristic is different for the two directions perpendicular to the orbit. Similar to the

Table 2: Total binding energies E and effective quantum number $n_{eff} = 1/\sqrt{E}$ for $^1S^e$ states obtained by WKB quantization of the fundamental orbit '$-$', by the cycle expansion, and by full quantum solutions (taken from Ref. [5].).

		N_{eff}			Energies	
$(n_\lambda, n_\mu)_\nu$	$(Nl, N'l')$	WKB	Cycle exp.	QM	Cycle exp.	QM
$(0,0)_0$	1s1s	0.568	0.584	0.587	2.932	2.904
$(0,2)_0$	2s2s	1.115	1.134	1.134	0.778	0.778
$(0,2)_1$	2s3s		1.308	1.302	0.585	0.590
$(0,4)_0$	3s3s	1.662	1.684	1.682	0.353	0.354
$(0,4)_1$	3s4s		1.883	1.886	0.282	0.281
$(0,6)_0$	4s4s	2.208	2.243	2.231	0.199	0.201
$(0,6)_1$	4s5s		2.456	2.456	0.166	0.166
$(0,6)_2$	4s6s		2.574	2.575	0.151	0.151
$(0,8)_0$	5s5s	2.755	2.783	2.780	0.129	0.129
$(0,8)_1$	5s6s		3.025	3.020	0.109	0.110
$(0,8)_2$	5s7s		3.154	3.159	0.101	0.100
$(0,10)_0$	6s6s	3.302	3.343	3.329	0.0895	0.0902
$(0,10)_1$	6s7s		3.586	3.580	0.0778	0.0780
$(0,10)_2$	6s8s		3.733	3.733	0.0717	0.0718
$(0,12)_0$	7s7s	3.849	3.903	3.883	0.0657	0.0663
$(0,12)_1$	7s8s		4.140	4.138	0.0583	0.0584
$(0,12)_2$	7s9s		4.305	4.301	0.0540	0.0541
$(0,14)_0$	8s8s	4.395	4.429	4.411	0.0510	0.0514
$(0,14)_1$	8s9s		4.689	4.686	0.0455	0.0455
$(0,14)_2$	8s10s		4.865	4.865	0.0423	0.0423

treatment for the (doubly) stable frozen planet orbit we identify m as a semiclassical quantum number for the stable bending degree of freedom. For the expansion of the remaining product we set the bookkeeping index j to $(2k+1)$ times the symbol length of the PO. The present calculations are carried out including all orbit contributions up to $j = 6$. In Table 2 we show our results for some doubly excited $^1S^e$ states with $m = 0$. For labeling the states we use the molecular-orbital (MO) classification $(n_\lambda, n_\mu)_\nu$ derived from an adiabatic treatment of the inter-electron vector $\mathbf{R}$ [14]. The MO quantum numbers accurately describe the nodal surfaces of the quantal wave functions for fixed inter-electron distances and moderate electron excitations ($N, N' < 6$). For convenience, we also give the "independent particle" labeling $(Nl, N'l')$, i.e. the configuration which would comes closest in an independent particle description. Here, $N, N' \geq N$ roughly correspond to the principal quantum numbers of the electrons.

It is more natural to compare the effective quantum numbers $N_{\rm eff} = E^{-1/2}$ than the binding energies E themselves, but both values are given in the table. We find that the cycle expansion results are mostly good to within 1% or better. This is better than might be expected.

In Table 2 we also list the results of the simplest cycle approach including only the fun-

damental PO '$-$', which is nothing but a WKB quantization of the orbit (but including the zero-point motion for the perpendicular degrees of freedom). Quantization of this fundamental asymmetric stretch PO gives rather accurate results for the doubly excited *intra-shell resonances* $N = N'$. These results and an analysis of the corresponding wavefunctions indicate that the intra-shell resonances are associated with the asymmetric stretch like motion of the fundamental PO '$-$' rather than the symmetric stretch motion along the Wannier ridge. This conclusion is in striking contrast to the common viewpoint expressed in the literature (see, e.g., Refs. [12]), but in line with recent suggestions [2, 7].

4. Conclusions

At present, semiclassical theories undergo a rapid and exciting evolution. In this contribution we applied many of the new ideas to the problem of two-electron atoms.

We are certainly at the beginning of refining the semiclassical methods for multi-dimensional methods like the PO-quantization approach. Further developments will probably include the description of dynamical tunneling processes. Other methods than the cycle expansion which drastically reduce the (exponentially growing) classical input of the semiclassic PO-quantization are also highly desirable.

References

[1] M. C. Gutzwiller, *Chaos in Classical and Quantum Mechanics* (Springer, New York, 1990); *J. Math. Phys.* **8**, 1979 (1967); **10**, 1004 (1969); **11**, 1791 (1970); **12**, 343 (1971).

[2] K. Richter and D. Wintgen, *J. Phys. B* **23**, L197 (1990).

[3] K. Richter, J. S. Briggs, D. Wintgen, and E. A. Solovév *J. Phys. B* **25**, 3929 (1992).

[4] K. Richter and D. Wintgen, *Phys. Rev. Lett.* **65**, 1965 (1990).

[5] G. S. Ezra, K. Richter, G. Tanner, and D. Wintgen, *J. Phys. B* **24**, L413 (1991)

[6] M. Domke, C. Xue, A. Puschmann, T. Mandel, E. Hudson, D. A. Shirley, G. Kaindl, C. H. Greene, H. R. Sadeghpour, H. Petersen, *Phys. Rev. Lett.* **66**, 1306 (1991).

[7] J.-H. Kim and G. S. Ezra, in *Proc. Adriatico Conf. on Quantum Chaos*, eds. H. Cerdeira *et al.* (World Scientific, Singapore, 1991).

[8] B. Eckhardt and D. Wintgen, *J. Phys. B* **23**, 355 (1990).

[9] B. Eckhardt and D. Wintgen, *J. Phys. A* **24**, 4335 (1991).

[10] A. Voros, *J. Phys. A* **21**, 685 (1988).

[11] R. Artuso, E. Aurell, and P. Cvitanović, *Nonlinearity* **3**, 325 and 361 (1990).

[12] A. R. P. Rau, *J. Phys. B* **16**, L699 (1983).

[13] H. R. Sadeghpour, *Phys. Rev. A* **43**, 5821 (1991).

[14] J. M. Rost and J. S. Briggs, *J. Phys. B* **24**, 4293 (1991).